

A Learned Cost Model-based Cross-engine Optimizer for SQL Workloads

András Strausz
IBM Research
Switzerland
andras.strausz@zurich.ibm.com

Niels Pardon
IBM Research
Switzerland
par@zurich.ibm.com

Ioana Giurgiu
IBM Research
Switzerland
igi@zurich.ibm.com

ABSTRACT

Lakehouse systems enable the same data to be queried with multiple execution engines. However, selecting the engine best suited to run a SQL query still requires a priori knowledge of the query’s computational requirements and an engine’s capabilities, a complex and manual task that only becomes more difficult with the emergence of new engines and workloads. In this paper, we address this limitation by proposing a cross-engine optimizer that can automate engine selection for diverse SQL queries through a learned cost model. Optimized with hints, a query plan is used for query cost prediction and routing. Cost prediction is formulated as a multi-task learning problem, and multiple predictor heads, corresponding to different engines and provisionings, are used in the model architecture. This eliminates the need to train engine-specific models and allows the flexible addition of new engines at a minimal fine-tuning cost. Results on various databases and engines show that using a query’s optimized logical plan for cost estimation decreases the average Q-error by even 12.6% over using unoptimized plans as input. Moreover, the proposed cross-engine optimizer reduces the total workload runtime by up to 25.2% in a zero-shot setting and 30.4% in a few-shot setting when compared to random routing.

PVLDB Reference Format:

András Strausz, Niels Pardon, and Ioana Giurgiu. A Learned Cost Model-based Cross-engine Optimizer for SQL Workloads. PVLDB, 14(1): XXX-XXX, 2024.
doi:XX.XX/XXX.XX

PVLDB Artifact Availability:

The source code, data, and/or other artifacts have been made available at <https://github.com/strausza-ibm/cross-engine-optim-artifacts>.

1 INTRODUCTION

Data has gone from being scarce to being super-abundant. Never before has it been so easy to collect large data quantities, due to the large-scale infrastructures available in the cloud. However, the increasing workload diversity in modern use-cases (i.e., lately seeking to harness unstructured data to fuel AI innovations) has led to the proliferation of specialized data management systems, each targeted to narrow types of workloads. For example, Postgres excels at executing SELECT queries by using indices, but significantly lags

behind Spark for general-purpose batch processing where parallel full scans are key. Presto is built for ad-hoc and interactive workloads, whereas Spark pays the penalty of always having to span and shut down workers as soon as workloads start or finish.

This has led to siloed systems, high maintenance costs and wasted engineering cycles. Even worse, the byproducts of this fragmentation – incompatible APIs, disparate functionality, inconsistent semantics – impact the end users, who commonly need to interact with multiple distinct systems to complete their tasks and to have expert knowledge to use them appropriately.

To alleviate some of these caveats, data management systems have seen a significant shift, from monolithic designs to modular approaches. Recent studies [12, 24] conceptualize a composable data system constructed from multiple independent layers: (1) the user-facing APIs, (2) the optimization layer, (3) the execution layer, and (4) the storage layer. Such cross-platform systems are horizontally extendable, making it easy to include various execution engines or storage systems and to express workloads in different dialects. However, how and where to execute these workloads in a cost/performance-optimal manner remains highly challenging.

Contributions. To overcome the above limitation, we propose optimizing engine selection in a lakehouse for SQL workloads through a learned cost model (LCM). The optimizer first applies traditional query-rewriting techniques to supply an optimized logical plan to the LCM, which we show to be beneficial for the downstream tasks of query cost prediction and routing. Cost prediction is formulated as a multi-task learning problem, using a Graph Neural Network (GNN) architecture to compute a general query representation. The resulting embedding is shared among multiple predictor heads corresponding to different engines and their respective provisionings, thus eliminating the need to train engine-specific LCMs.

The optimizer is evaluated in a lakehouse system with five different engine configurations on various synthetic and real-world databases (DBs). In a zero-shot setting, its query-to-engine routing reduces the workload total runtime by up to 25.2% over a random routing. In a few-shot setting, results are even better and the optimizer’s routing outperforms random routing by even 30.4%. These improvements translate to tens of minutes saved in execution even for small databases, such as IMDB or TPC-H. Lastly, experiments on introducing a new engine provisioning showcase the optimizer’s ability to flexibly add a new predictor head in the LCM at a cheap fine-tuning cost, by training it only on 250 queries.

2 BACKGROUND

Polystores and Federated Data Management Systems. In line with our objective, polystores [2, 4, 10, 25, 30, 37] and federated DBs [7, 14, 26, 35] also aim to distribute query workloads across

This work is licensed under the Creative Commons BY-NC-ND 4.0 International License. Visit <https://creativecommons.org/licenses/by-nc-nd/4.0/> to view a copy of this license. For any use beyond those covered by this license, obtain permission by emailing info@vldb.org. Copyright is held by the owner/author(s). Publication rights licensed to the VLDB Endowment.
Proceedings of the VLDB Endowment, Vol. 14, No. 1 ISSN 2150-8097.
doi:XX.XX/XXX.XX

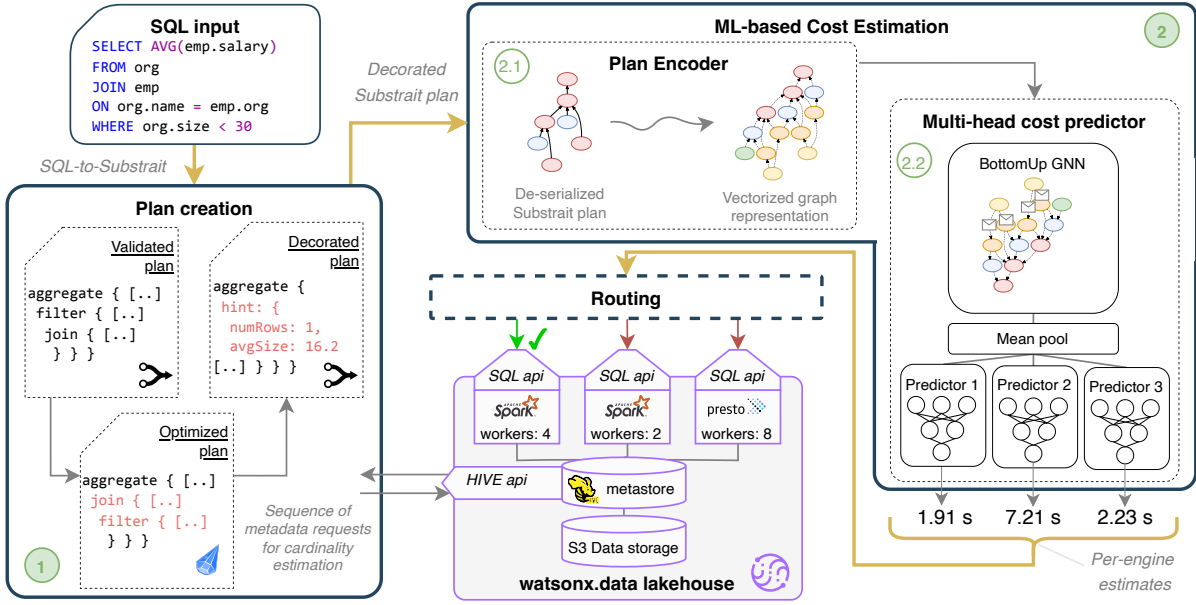


Figure 1: Overview of the cross-engine optimizer.

heterogeneous engines. Specifically, they optimize queries within a given set of engines and hardware configurations. For example, RHEEM [2] requires additional work to specify selectivity and cost templates for each operator when including a new engine, which can quickly become a burden for extension. In contrast, we enable the easy addition of a new engine to the underlying infrastructure to support the user’s workload.

LCMs for Query Optimization and Cost Estimation. Recently, LCMs [5, 8, 15, 20, 21, 23, 32, 38, 39] that aim to learn and enhance the behavior of the DB engine’s optimizer have been proposed. Some [5, 20, 23] use the traditional optimizer’s hints to improve the optimization procedure. Others [8, 21, 32, 38] attempt to fully replace the query optimizer with a learned query rewriter. Finally, a variety of approaches [13, 31, 33] estimate query cost with LCMs. Stage [31] proposes a hierarchical modeling strategy, where either instance-level or global models are used for the task. For the latter, the Graph Neural Network (GNN) architecture described in [13] is used. Similarly, BRAD [33] uses the same architecture to tackle query-to-engine routing. To select the cost-optimal engine, it considers multiple cost factors, some estimated by closed-form functions, and others by learned models. Most importantly, for execution time prediction, it uses unoptimized logical query plans. Each execution engine is considered separately, so an individual predictor model would need to be trained for each. While we are inspired by the bottom-up GNN architecture, we propose a multi-head predictor that simultaneously predicts execution times for all supported engines and allows new engines to be easily added by fine-tuning a new predictor head on a small volume of queries.

LCM Architectures. Various architectures have been explored for LCMs, ranging from flat vectors [11, 16] with Multi Layer Perceptrons (MLP), to Tree Convolutional Networks [22], Recurrent Neural Networks [29, 34] and Transformer models [36]. More recently,

GNNs have gained popularity due to their natural representation of query structures. A message passing algorithm over the query execution plan has been proposed in [13]. Similarly to sequence models, by adjusting the message passing order to follow the execution plan’s topology, nodes receive information from their subtree. Thus, the computed hidden embedding of a node is a representation of this subtree. Consequently, the root node’s embedding can be used as a representation of the complete input graph. Embeddings are computed using node-specific MLPs, and messages are aggregated by summing. Finally, LLMs have been used to embed the query text [3], because of their understanding of predicated or even complete SQL statements. These embeddings can be used either as a complement to other query or predicate embeddings computed using numeric features or even as standalone representations.

3 CROSS-ENGINE OPTIMIZER

The cross-engine optimizer acts as a middleware and interacts with the underlying system’s engines and metadata provider in a lakehouse. Its objective is, upon receiving a user query, to estimate the query’s execution time on each engine using an LCM and then use those for engine selection.

The architecture of the cross-engine optimizer is shown in Figure 1. The input query is first received by the ① *Plan creation* module, which transforms it into an optimized Substrait [28] plan with cardinality hints. This plan is forwarded to the ② *ML-based cost-estimation* module, which encodes the deserialized plan and predicts the query’s execution time for each engine. Finally, these predictions are used for *Routing*.

3.1 Plan Creation

During plan creation ①, the SQL query is transformed into an optimized Substrait plan with hints containing cost-related information

Algorithm 1 Multi-task predictor with Bottom-up GNN encoder

```

1: Input: vectorized query graph  $\mathbf{x}$ , set of engines  $\mathcal{E}$ 
2: Output: per-engine execution time prediction
3: # Create query graph embedding using Bottom-up GNN
4: for  $v \in$  input graph do
5:    $\mathbf{h}_v \leftarrow \text{EncoderMLP}_T(\mathbf{x}_v)$ 
6: for  $v \in$  topological order do
7:    $\mathbf{h}'_v \leftarrow \text{HiddenMLP}_T(\sum_{u \in \text{children}(v)} \mathbf{h}'_u \oplus \mathbf{h}_v)$ 
8: # Mean-pool over embeddings of Relation nodes
9:  $\mathbf{h}_{\text{query}} \leftarrow \text{mean\_pool}(\{\mathbf{h}'_v : v \in \text{Relation}\})$ 
10: # Prediction using separate predictor heads
11: for  $i \in 1 \dots |\mathcal{E}|$  do
12:    $\hat{y}[i] \leftarrow \text{PredictorMLP}_i(\mathbf{h}_{\text{query}})$ 
13: return  $\hat{\mathbf{y}}$ 

```

For *Operation* and *Relation* nodes, the featurization also includes the type of the expression (such as Join, Filter for *Relation* or max, +, -, etc. for *Operation*) as a one-hot encoded vector. For *Relation*, each relation included in the Substrait specification is represented as a distinct category. *Operation* expressions are assigned to categories via a predefined static mapping that groups expressions with similar computational complexity. Log-normalization is applied to all continuous features to avoid large differences in scale between features. Table 1 lists the features considered for each node type and Figure 2 depicts an example output of the featurization process.

3.2.2 LCM architecture. The multi-head cost predictor (2.2) first employs a GNN to convert the encoded query plan into a low-dimensional embedding. This embedding is fed into each predictor head, producing an execution time estimate for the respective execution engine. The embedding heads are implemented as Multi-layer Perceptrons (MLPs). Algorithm 1 provides pseudo code for the multi-task inference process.

The algorithm first projects nodes in the input graph to a common vector space using type-specific encoders. In particular, for each node with type $T \in \{\text{Relation}, \text{Operation}, \text{Literal}, \text{Field}, \text{Table}\}$, the corresponding encoder $\text{EncoderMLP}_T : \mathbb{R}^{d_T} \rightarrow \mathbb{R}^{d'}$ is applied (lines 4-5). Afterwards, in the message passing phase, messages are propagated through the tree in topological order, starting from leaf nodes and progressing towards the last *Relation* node. At each step, nodes send messages to their parent nodes once they have received all messages from their children. After a node receives messages, it updates its hidden embedding by first concatenating it to the sum of received embeddings and feeding this combined embedding through a second, type-specific MLP, $\text{HiddenMLP}_T : \mathbb{R}^{d'+d'} \rightarrow \mathbb{R}^{d'}$ (lines 6-7). The mean-pooling operation is then applied over all *Relation* nodes in the graph (line 9) to arrive at the final, learned representation of the query. This representation is then received by the engine-specific predictor heads, $\text{PredictorMLP}_i : \mathbb{R}^{d'} \rightarrow \mathbb{R}$ to compute the final estimates.

Let $\mathcal{E} = \{e_1, \dots, e_{|\mathcal{E}|}\}$ be a set of engines. For a query \mathbf{x} , encoded in a vectorized graph format, we record corresponding measurements $\mathbf{y} \in \mathbb{R}^{|\mathcal{E}|}$, where the i -th component $y[i]$ is the execution time of the query measured on engine e_i . Furthermore, let $\text{BottomUpGNN}(\mathbf{x}) : \mathcal{G} \rightarrow \mathbb{R}^{d'}$ represent the complete bottom-up

	Raw Size (GB)	Parquet Size (GB)	#Tables	#Rows (M)	#Rel
TPC-H	10	3.2	8	86.6	8
TPC-DS	10	4.2	24	191.5	102
IMDB	3.6	1.8	23	74.3	17
Stack Overflow	4.4	2.1	9	19.3	12
Donor	1.7	0.75	4	7.5	4

Table 2: Summary of datasets. #Rel is the number of foreign-key constraints taken into account for query generation.

message passing algorithm, including mean-pooling (lines 4-9) and producing a d' -dimensional embedding of the input graph. During training, each task (i.e., predicting the execution time for a specific engine configuration) is weighted equally. Namely, for a loss function $\mathcal{L}(\cdot, \cdot)$ between predicted and measured execution time, we compute the prediction error for backpropagation as:

$$l = \frac{1}{|\mathcal{E}|} \sum_{i \in \{1, \dots, |\mathcal{E}|\}} \mathcal{L}(\text{PredictorMLP}_i(\text{BottomUpGNN}(\mathbf{x})), y[i])$$

During training, an adjusted form of Q-error is employed as the loss function, computing the standard Q-error for positive estimates and assigning an arbitrarily large penalty for negative estimates.

4 EVALUATION

4.1 Methodology

4.1.1 Environment. All experiments have been conducted on a cluster with dual-socket compute nodes, each hosting 2 Intel Xeon E5-2683 v4 CPUs and 768GB of RAM. The cluster is running on OpenShift, where the watsonx.data [1] lakehouse is hosted. Since watsonx.data currently natively supports only PrestoDB and SparkSQL, we evaluate on these 2 engine types with 4 provisionings (1 and 4 worker nodes, respectively). Furthermore, all caching capabilities of PrestoDB are disabled to ensure that measurements are independent. Data is stored in MinIO buckets in parquet format, and a Hive catalog is used to keep and distribute metadata inside the lakehouse. For the experiment introducing a new engine, a PrestoDB provisioning with 8 worker nodes is considered.

4.1.2 Data Collection. 5 different datasets were selected for evaluation: TPC-H and TPC-DS with a scale factor of 10, the IMDB dataset from the JOB [17], a one-year data dump of Stack Overflow and the donor dataset from the BIRD-SQL benchmark [18]. Each dataset contains multiple foreign key relationships and column types, ranging from simple numeric and text values to dates and timestamps. Some of the key statistics of the datasets are summarized in Table 2.

Since traditional benchmarks include at most a few hundred queries, insufficient for the LCM training, we use the synthetic query generator from [13]. Following prior works, queries are limited to at most 3 joins and a maximum runtime of 1 minute to allow efficient training data collection. However, the generated queries include predicates on timestamp and date columns as well as subqueries and predicates on aggregates (HAVING statements). As our cross-engine optimizer relies on Calcite’s grammar-driven SQL parser and its featurization process covers the full range of relations and data types defined by Substrait, this is the first attempt to support such a broader spectrum of queries systematically.

GNN:	EncoderMLP _T :	(<i>input_dim</i> , 64, 96, 144, 216, 256) × 5
	HiddenMLP _T :	(512, 384, 384, 384, 256) × 5
	PredictorMLP _e :	(256, 174, 121, 85, 59, 1) × #engines
Set-based:	EncoderMLP _T :	(<i>input_dim</i> , 64, 96, 144, 216, 256) × 5
	PredictorMLP _e :	(1024, 174, 121, 85, 59, 1) × #engines

Table 3: Layer sizes of each MLP used for the GNN and set-based architectures. *input_dim* refers to the encoded dimension (number of features) of each node type.

	Q _{med}	Q _{mean}	Q _{p95}
Ours	<u>1.21</u>	<u>1.47</u>	<u>2.43</u>
GNN.UP	1.24	1.55	2.71
SB.OP	<u>1.21</u>	<u>1.47</u>	2.45

Table 4: Unseen queries: prediction accuracy on unseen queries.

For each dataset, 5000 queries are generated and executed on each execution engine.

4.1.3 Evaluation Scenarios. To thoroughly evaluate both the proposed LCM’s accuracy in predicting execution time and its effectiveness for routing queries, we consider 4 scenarios:

- (1) *Unseen queries*: all 5 datasets are merged for training and testing. For evaluation, 1000 queries are held out from each dataset.
- (2) *Zero-shot*: the LCM is evaluated on a dataset excluded from training. We report cross-validation results in which, for each fold, 4 datasets serve as the training set and the fifth is used for evaluation.
- (3) *Few-shot*: the LCM is fine-tuned on a small subset of queries drawn from the test dataset. Only the predictor heads are updated, while the shared embedding model remains fixed. We use 250 (~5%) queries for few-shot experiments, split equally between training and validation.
- (4) *New engine*: a new predictor head is trained for the new engine in a few-shot setting. This scenario addresses the case where the current provisioning is insufficient for running the workload under a preferred time or cost budget.

4.2 Results on LCM’s Accuracy

We begin by analyzing the proposed LCM’s estimation accuracy in each scenario, using the Q-error metric, averaged over all considered engines. The metric Q_{med} for a set of queries Q and a set of engines \mathcal{E} is computed as:

$$Q_{med} = \frac{1}{|\mathcal{E}|} \sum_{i \in 1 \dots |\mathcal{E}|} median \left(\left\{ \max \left(\frac{pred_q}{true_q}, \frac{true_q}{pred_q} \right) : q \in Q \right\} \right)$$

Results for IMDB, Stack Overflow and TPC-H are presented below. Appendix 6.2 includes the evaluation of the remaining datasets.

4.2.1 Baselines. We define 2 baselines to compare against:

- (1) *GNN.UP*: the LCM is trained with *validated plans* and no optimizations. Specifically, input plans are produced by applying field trimming to the original Substrait plan and converting subqueries into joins. This baseline is closest to BRAD [33], which creates the input graph directly from the SQL text.
- (2) *SB.OP*: we implement an adjusted version of the set-based model proposed by Kipf et al. [16] with optimized plans. Details are provided in Appendix 6.1.

	IMDB			Stack Overflow			TPC-H		
	Q _{med}	Q _{mean}	Q _{p95}	Q _{med}	Q _{mean}	Q _{p95}	Q _{med}	Q _{mean}	Q _{p95}
Ours	<u>1.51</u>	<u>1.81</u>	<u>3.57</u>	<u>1.44</u>	<u>1.95</u>	<u>4.23</u>	<u>1.40</u>	<u>1.71</u>	<u>3.16</u>
GNN.UP	1.67	2.07	4.36	1.45	1.95	4.35	1.49	1.84	3.52
SB.OP	1.53	1.90	4.13	1.47	1.97	4.26	1.43	1.80	3.32

Table 5: Zero-shot: prediction accuracy of zero-shot models.

	IMDB			Stack Overflow			TPC-H		
	Q _{med}	Q _{mean}	Q _{p95}	Q _{med}	Q _{mean}	Q _{p95}	Q _{med}	Q _{mean}	Q _{p95}
Ours	1.37	1.56	2.76	1.35	1.73	3.42	1.29	1.55	2.70
GNN.UP	1.45	1.73	3.42	1.43	1.87	3.99	1.31	1.63	2.87
SB.OP	<u>1.37</u>	<u>1.57</u>	<u>2.72</u>	1.38	1.82	3.64	<u>1.29</u>	<u>1.59</u>	<u>2.63</u>

Table 6: Few-shot: prediction accuracy of few-shot models.

4.2.2 Results on unseen queries. Evaluating on queries targeting the same underlying databases as those used for training leads to generally accurate predictions, as reported in Table 4. Note that a median Q-error of 1.21, which is achieved for both our proposed model and for the set-based architecture, means that, on average over each predictor head, 50% of the estimates deviate by no more than 21% from the true, measured execution time.

Comparing optimized and unoptimized plans with the GNN architecture, we see a 5.2% relative reduction in Q_{mean} and a 10.3% reduction in the tail error Q_{p95} in favor of optimized plans. These results reinforce the idea that the input plans for the LCM can be improved through traditional query optimization techniques. The differences between model architectures are minor and only present in the tail error by a 0.2 difference in Q_{p95} . Thus, in this scenario, the GNN architecture cannot extract a considerably larger amount of additional information from the plan’s structure compared to the simpler set-based model. Furthermore, the accuracy of different predictor heads shows only low variance. This implies that the learned embedding, whether created by the GNN or the set-based model, is general enough to be used for predicting execution times on different engines.

4.2.3 Results for zero-shot setting. Results are reported in Table 5. Zero-shot models exhibit substantially higher Q-errors than models trained and evaluated on the combined dataset. Nevertheless, similar trends are observed in the zero-shot setting, where query optimization also yields more accurate predictions compared with those obtained using unoptimized plans. In particular, using optimized plans with the GNN architecture improves on the average Q-error by 9.6% and by 18.2% in Q_{p95} for the IMDB dataset over using unoptimized plans. On the other hand, results for the Stack Overflow dataset show a difference only in the tail error. For this dataset, all considered settings lead to similar metrics, and generally high tail error. We also observe that the GNN architecture generalizes better than the set-based model, achieving superior results on all but one dataset.

4.2.4 Results on few-shot setting. The few-shot setting is designed to enable the predictor heads to capture dataset-specific cost characteristics by fine-tuning and thus produce more accurate predictions. Comparing the few-shot results (Table 6) with the zero-shot results shows that fine-tuning indeed improves the LCM’s accuracy, as reflected by improvements in each metric across all configurations.

	IMDB			Stack Overflow			TPC-H		
	q_{med}^{Pw8}	q_{mean}^{Pw8}	q_{p95}^{Pw8}	q_{med}^{Pw8}	q_{mean}^{Pw8}	q_{p95}^{Pw8}	q_{med}^{Pw8}	q_{mean}^{Pw8}	q_{p95}^{Pw8}
Ours	1.54	1.74	3.11	1.43	1.80	3.37	1.27	1.50	2.40
GNN.UP	1.55	1.90	3.89	1.44	1.86	3.73	1.31	1.58	2.57
SB.OP	1.47	1.72	3.18	1.46	1.87	3.58	1.32	1.54	2.54

Table 7: New engine: prediction accuracy of the new predictor.

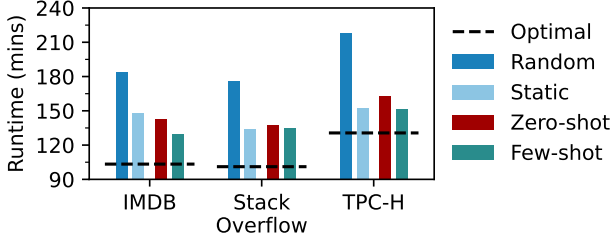


Figure 3: Query-level routing using our proposed LCM.

Significant reductions in the Q-error (between 20% and 40%) are observed particularly in the tail error.

4.2.5 Results on adding a new engine. Finally, Table 7 shows the Q-error of the LCM after including a new predictor head that represents an additional engine provisioning (*PrestoW8*) in the lakehouse. Recall that the new predictor head is only trained using 250 queries, keeping the cost of data collection low, as well as the training cost. Overall, we observe metrics for each dataset that closely match those from the few-shot experiments. This demonstrates that the learned embedding allows for including a new predictor for an engine different than those used in the LCM pre-training.

4.3 Effect on Query Execution Times and Routing

We analyze the LCM’s effect on query-level routing both in the *zero-shot* and *few-shot* scenarios. Each query is assigned to the execution engine, which is estimated to lead to the shortest execution time.

4.3.1 Baselines. Two baselines are considered for query routing: (1) *Random*: the engine is selected randomly for each query. (2) *Static*: the complete workload is executed on the engine that minimizes the workload’s total runtime. Note that this routing requires a priori knowledge in determining which engine should be used for execution.

4.3.2 Results. Figure 3 shows the total execution time of the considered workloads under different routing strategies. In the *zero-shot* setting, relying on the LCM for engine selection reduces total runtime by up to 25.3% over a random routing, corresponding to a 54.9 minute difference. The improved estimation accuracy in the *few-shot* scenario also translates to more accurate routing. Specifically, using a *few-shot* predictor reduces total runtime over random routing by 54.4 minutes (−29.7%) for IMDB, 41.8 minutes (−23.7%) for Stack Overflow, and 66.1 minutes (−30.4%) for TPC-H. Finally, the fine-tuned predictors also lead to similar or lower total execution time compared to static routing. For instance, on the IMDB dataset, the difference between the LCM-based and static routing grows to 18.8 minutes (12.7%) in favor of the LCM.

We remark the significant differences compared to random routing, despite the fact that queries are short-running (<1 minute) and thus limit the gains from engine selection. Scaling data sizes and raising the timeout threshold will likely offer further improvements.

4.4 LCM Training

Finally, Table 3 summarizes the intermediate sizes of each MLP used in the GNN and set-based model. The resulting GNN has a total of 4.7M parameters, whereas the set-based model consists of 1.6M parameters. The models are trained with the AdamW optimizer [19] and a learning rate of 0.001 for at least 200 epochs, using early stopping with a patience of 25 epochs. From each dataset considered for training, 250 queries are reserved for validation.

Using a single NVIDIA Tesla V100-SXM2 32GB GPU, the training on the complete dataset (~17k datapoints in the training set) takes around 7 hours for the GNN and 3 hours for the set-based model. The fine-tuning process for few-shot takes ~10min for the GNN model and ~5min for the set-based model. Finally, the inference time on GPU for a single query is ~4.5 ms with the GNN architecture and ~0.7 ms with the set-based.

5 CONCLUSIONS

In this paper, we have presented a cross-engine optimizer for executing SQL workloads in lakehouse systems, which automates the engine selection process. This has the benefit of simplifying the lakehouse architecture and presenting it to the user as a single-endpoint interface. We have shown that combining traditional query optimization techniques with an LCM leads to enhanced prediction accuracy due to the more accurate query plan representation received and learned by the LCM. Furthermore, we proposed to formulate cost prediction across multiple engines as a multi-task learning problem, thereby avoiding the need to train engine-specific cost models and flexibly supporting the inclusion of new engine instances at a low cost.

We identify the random query generation as the main limitation, as it only provides weak control over the nature of the generated queries, both in terms of their complexity and their semantic plausibility. For example, in some cases, random predicate combinations often filter out most or even all of the data early, producing near-empty joins. In other cases, queries become full-table joins, leading to long execution times. We believe that with the increasing availability of publicly accessible real-world databases, one can design a synthetic query generator that produces a larger diversity of meaningful queries, with varying degrees of complexity. Such a query generator could then be further integrated with the cost estimator, such that the LCM’s past estimation errors can guide the query generation process via reinforcement learning techniques.

In the future, we also plan to enhance the LCM with cost aspects around engine provisioning, storage, data movement, and engine load, making the routing decision more informed. Furthermore, we aim to adjust the modeling approach to estimate node-level cost and include this in an optimizer for the distributed execution of SQL queries.

REFERENCES

- [1] 2025. IBM watsonx.data. <https://www.ibm.com/docs/en/watsonx/watsonxdata/2.1.x?topic=overview>
- [2] Divy Agrawal, Sanjay Chawla, Bertty Contreras-Rojas, Ahmed Elmagarmid, Yasser Idris, Zoi Kaoudi, Sebastian Kruse, Ji Lucas, Essam Mansour, Mourad Ouzzani, Paolo Papotti, Jorge-Arnulfo Quiané-Ruiz, Nan Tang, Saravanan Thirumuruganathan, and Anis Troudi. 2018. RHEEM: enabling cross-platform data processing: may the big data be with you! *Proceedings of the VLDB Endowment* 11, 11 (July 2018), 1414–1427. <https://doi.org/10.14778/3236187.3236195>
- [3] Peter Akiyamen, Zixuan Yi, and Ryan Marcus. 2024. The Unreasonable Effectiveness of LLMs for Query Optimization. <https://doi.org/10.48550/arXiv.2411.02862> arXiv:2411.02862 [cs].
- [4] Rana Alotaibi, Damian Bursztyn, Alin Deutsch, Ioana Manolescu, and Stamatis Zampetakis. 2019. Towards Scalable Hybrid Stores: Constraint-Based Rewriting to the Rescue. In *2019 International Conference on Management of Data*. ACM, 1660–1677. <https://doi.org/10.1145/3299869.3319895>
- [5] Christoph Anneser, Nesime Tatbul, David Cohen, Zhenggang Xu, Prithviraj Pandian, Nikolay Laptev, and Ryan Marcus. 2023. AutoSteer: Learned Query Optimization for Any SQL Database. *Proceedings of the VLDB Endowment* 16, 12 (Aug. 2023), 3515–3527. <https://doi.org/10.14778/3611540.3611544>
- [6] Edmon Begoli, Jesús Camacho Rodríguez, Julian Hyde, Michael J. Mior, and Daniel Lemire. 2018. Apache Calcite: A Foundational Framework for Optimized Query Processing Over Heterogeneous Data Sources. In *Proceedings of the 2018 International Conference on Management of Data*. 221–230. <https://doi.org/10.1145/3183713.3190662> arXiv:1802.10233 [cs].
- [7] Yuri Breitbart, Hector Garcia-Molina, and Avi Silberschatz. 1992. Overview of Multidatabase Transaction Management. In *VLDB Journal*, vol. 1, no. 2. ACM, 181–239.
- [8] George-Octavian Bărbulescu, Taiyi Wang, Zak Singh, and Eiko Yoneki. 2024. Learned Graph Rewriting with Equality Saturation: A New Paradigm in Relational Query Rewrite and Beyond. <http://arxiv.org/abs/2407.12794> arXiv:2407.12794 [cs].
- [9] Rich Caruana. [n.d.]. Multitask Learning. ([n. d.]).
- [10] Vijay Gadepally, Peinan Chen, Jennie Duggan, Aaron Elmore Elmore, Brandon Haynes, Jeremy Kepner Kepner, Samuel Madden Madden, Tim Mattson Mattson, and Michael Stonebraker. 2015. The BigDAWG Polystore System. In *ACM SIGMOD Record*, vol. 44, no. 2. ACM, 11–16.
- [11] Archana Ganapathi, Harumi Kuno, Umeshwar Dayal, Janet L. Wiener, Armando Fox, Michael Jordan, and David Patterson. 2009. Predicting Multiple Metrics for Queries: Better Decisions Enabled by Machine Learning. In *2009 IEEE 25th International Conference on Data Engineering*. 592–603. <https://doi.org/10.1109/ICDE.2009.130> ISSN: 2375-026X.
- [12] Haralampos Gavrilidis, Lennart Behme, Sokratis Papadopoulos, Stefano Bortoli, Jorge-Arnulfo Quiané-Ruiz, and Volker Markl. [n.d.]. Towards a Modular Data Management System Framework. ([n. d.]).
- [13] Benjamin Hilprecht and Carsten Binnig. 2022. Zero-shot cost models for out-of-the-box learned cost prediction. *Proceedings of the VLDB Endowment* 15, 11 (July 2022), 2361–2374. <https://doi.org/10.14778/3551793.3551799>
- [14] Vanja Josifovski, Peter Schwarz Schwarz, Laura Haas Haas, and Eileen Lin. 2002. Garlic: A New Flavor of Federated Query Processing for DB2. In *2002 ACM SIGMOD International Conference on Management of Data*. ACM, 524–532.
- [15] Amin Kamali, Verena Kantere, Calisto Zuzarte, and Vincent Corvini. [n.d.]. Roq: Robust Query Optimization Based on a Risk-aware Learned Cost Model. ([n. d.]).
- [16] Andreas Kipf, Thomas Kipf, Bernhard Radke, Viktor Leis, Peter Boncz, and Alfons Kemper. 2018. Learned Cardinalities: Estimating Correlated Joins with Deep Learning. <https://doi.org/10.48550/arXiv.1809.00677> arXiv:1809.00677 [cs].
- [17] Viktor Leis, Andrey Gubichev, Atanas Mirchev, Peter Boncz, Alfons Kemper, and Thomas Neumann. 2015. How good are query optimizers, really? *Proceedings of the VLDB Endowment* 9, 3 (Nov. 2015), 204–215. <https://doi.org/10.14778/2850583.2850594>
- [18] Jinyang Li, Binyuan Hui, Ge Qu, Jiaxi Yang, Binhua Li, Bowen Li, Bailin Wang, Bowen Qin, Rongyu Cao, Ruiying Geng, Nan Huo, Xuanhe Zhou, Chenhao Ma, Guoliang Li, Kevin C. C. Chang, Fei Huang, Reynold Cheng, and Yongbin Li. 2023. Can LLM Already Serve as A Database Interface? A Big Bench for Large-Scale Database Grounded Text-to-SQLs. <https://doi.org/10.48550/arXiv.2305.03111> arXiv:2305.03111 [cs].
- [19] Ilya Loshchilov and Frank Hutter. 2019. Decoupled Weight Decay Regularization. <https://doi.org/10.48550/arXiv.1711.05101> arXiv:1711.05101 [cs].
- [20] Ryan Marcus, Parimarjan Negi, Hongzi Mao, Nesime Tatbul, Mohammad Alizadeh, and Tim Kraska. 2021. Bao: Making Learned Query Optimization Practical. In *Proceedings of the 2021 International Conference on Management of Data*. ACM, Virtual Event China, 1275–1288. <https://doi.org/10.1145/3448016.3452838>
- [21] Ryan Marcus, Parimarjan Negi, Hongzi Mao, Chi Zhang, Mohammad Alizadeh, Tim Kraska, Olga Papaemmanouil, and Nesime Tatbul. 2019. Neo: a learned query optimizer. *Proceedings of the VLDB Endowment* 12, 11 (July 2019), 1705–1718. <https://doi.org/10.14778/3342263.3342644>
- [22] Lili Mou, Ge Li, Lu Zhang, Tao Wang, and Zhi Jin. 2015. Convolutional Neural Networks over Tree Structures for Programming Language Processing. <https://doi.org/10.48550/arXiv.1409.5718> arXiv:1409.5718 [cs].
- [23] Parimarjan Negi, Matteo Interlandi, Ryan Marcus, Mohammad Alizadeh, Tim Kraska, Marc Friedman, and Alekh Jindal. 2021. Steering Query Optimizers: A Practical Take on Big Data Workloads. In *Proceedings of the 2021 International Conference on Management of Data*. ACM, Virtual Event China, 2557–2569. <https://doi.org/10.1145/3448016.3457568>
- [24] Pedro Pedreira, Orri Erling, Konstantinos Karanasos, Scott Schneider, Wes McKinney, Satya R Valluri, Mohamed Zait, and Jacques Nadeau. 2023. The Composable Data Management System Manifesto. *Proceedings of the VLDB Endowment* 16, 10 (June 2023), 2679–2685. <https://doi.org/10.14778/3603581.3603604>
- [25] Maksim Podkorytov and Michael Gubanov. 2019. Hybrid.Poly: A Consolidated Interactive Analytical Polystore System. In *2019 IEEE 35th International Conference on Data Engineering (ICDE)*. IEEE, 1996–1999.
- [26] Calton Pu. 1998. Superdatabases for Composition of Heterogeneous Databases. In *Fourth International Conference on Data Engineering (ICDE)*. IEEE, 548–555.
- [27] P Griffiths Selinger, M M Astrahan, D D Chamberlin, R A Lorie, and T G Price. [n.d.]. Access Path Selection in a Relational Database Management System. ([n. d.]).
- [28] substraat-io. 2021. Substrait: Cross-Language Serialization for Relational Algebra. <https://github.com/substrait-io/substrait> original-date: 2021-08-31T21:40:13Z.
- [29] Ji Sun and Guoliang Li. 2019. An end-to-end learning-based cost estimator. *Proceedings of the VLDB Endowment* 13, 3 (Nov. 2019), 307–319. <https://doi.org/10.14778/3368289.3368296>
- [30] Marco Vogt, Alexander Stiemer, and Heiko Schuld. 2018. Polypheny-DB: Towards a Distributed and Self-Adaptive Polystore. In *2018 IEEE International Conference on Big Data (Big Data)*. IEEE, 3364–3373.
- [31] Ziniu Wu, Ryan Marcus, Zhengchun Liu, Parimarjan Negi, Vikram Nathan, Pascal Pfeil, Gaurav Saxena, Mohammad Rahman, Balakrishnan Narayanaswamy, and Tim Kraska. 2024. Stage: Query Execution Time Prediction in Amazon Redshift. <http://arxiv.org/abs/2403.02286> arXiv:2403.02286 [cs].
- [32] Zongheng Yang, Wei-Lin Chiang, Sifei Luan, Gautam Mittal, Michael Luo, and Ion Stoica. 2022. Balsa: Learning a Query Optimizer Without Expert Demonstrations. In *Proceedings of the 2022 International Conference on Management of Data*. ACM, Philadelphia PA USA, 931–944. <https://doi.org/10.1145/3514221.3517885>
- [33] Geoffrey X. Yu, Ziniu Wu, Ferdi Kossmann, Tianyu Li, Markos Markakis, Amadou Ngom, Samuel Madden, and Tim Kraska. 2024. Blueprinting the Cloud: Unifying and Automatically Optimizing Cloud Data Infrastructures with BRAD – Extended Version. *Proceedings of the VLDB Endowment* 17, 11 (July 2024), 3629–3643. <https://doi.org/10.14778/3681954.3682026> arXiv:2407.15363 [cs].
- [34] Xiang Yu, Guoliang Li, Chengliang Chai, and Nan Tang. 2020. Reinforcement Learning with Tree-LSTM for Join Order Selection. In *2020 IEEE 36th International Conference on Data Engineering (ICDE)*. IEEE, Dallas, TX, USA, 1297–1308. <https://doi.org/10.1109/ICDE48307.2020.00116>
- [35] Jianqiu Zhang, Kaisong Huang, Tianzheng Wang, and King Lv. 2022. Skeena: Efficient and Consistent Cross-Engine Transactions. In *2022 International Conference on Management of Data*. ACM, 34–48.
- [36] Yue Zhao, Gao Cong, Jiachen Shi, and Chunyan Miao. 2022. QueryFormer: a tree transformer model for query plan representation. *Proceedings of the VLDB Endowment* 15, 8 (April 2022), 1658–1670. <https://doi.org/10.14778/3529337.3529349>
- [37] Xiuwen Zheng, Subhasis Dasgupta, Arun Kumar Kumar, and Amarnath Gupta. 2022. AWESOME: Empowering Scalable Data Science on Social Media Data with an Optimized Tri-Store Data System. In <https://arxiv.org/pdf/2112.00833>.
- [38] Xuanhe Zhou, Guoliang Li, Chengliang Chai, and Jianhua Feng. 2021. A learned query rewrite system using Monte Carlo tree search. *Proceedings of the VLDB Endowment* 15, 1 (Sept. 2021), 46–58. <https://doi.org/10.14778/3485450.3485456>
- [39] Rong Zhu, Wei Chen, Bolin Ding, Xingguang Chen, Andreas Pfadler, Ziniu Wu, and Jingren Zhou. 2023. Lero: A Learning-to-Rank Query Optimizer. *Proceedings of the VLDB Endowment* 16, 6 (Feb. 2023), 1466–1479. <https://doi.org/10.14778/3583140.3583160>

6 APPENDIX

6.1 Set-based model

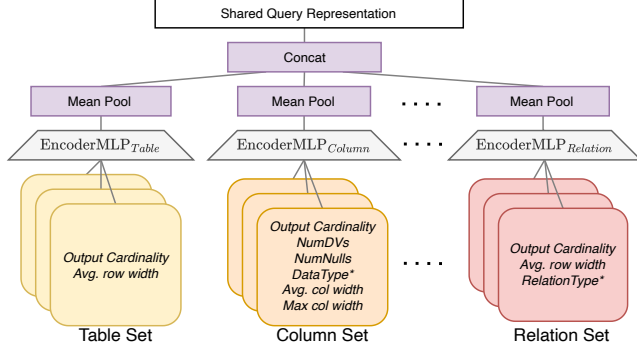


Figure 4: Set-based approach for query representation.

The *SB.OP* baseline is adjusted from Kipf et al. [16]. In particular, the same featurization process is employed as for the GNN architecture. However, each node belonging to the same type is treated as a set of objects, without their exact relationship being modeled. Analogous to the GNN, five sets are used for modeling, each corresponding to one of the considered node types. The resulting approach is depicted in Figure 4.

6.2 Results for TPC-DS and Donor

	TPC-DS			Donor		
	q_{med}	q_{mean}	q_{p95}	q_{med}	q_{mean}	q_{p95}
Ours	1.48	2.48	5.93	<u>1.59</u>	<u>1.98</u>	3.94
GNN.UP	1.55	2.37	5.93	1.84	2.12	4.09
SB.OP	<u>1.45</u>	<u>2.16</u>	<u>5.25</u>	1.70	2.00	<u>3.84</u>

Table 8: Zero-shot: prediction accuracy of zero-shot models.

	TPC-DS			Donor		
	q_{med}	q_{mean}	q_{p95}	q_{med}	q_{mean}	q_{p95}
Ours	1.32	2.28	5.15	<u>1.28</u>	<u>1.46</u>	<u>2.42</u>
GNN.UP	1.34	2.01	4.81	1.35	1.53	2.57
SB.OP	<u>1.31</u>	<u>1.86</u>	<u>3.91</u>	1.30	1.49	2.45

Table 9: Few-shot: prediction accuracy of few-shot models.

	TPC-DS			Donor		
	$q_{med}^{P_{w8}}$	$q_{mean}^{P_{w8}}$	$q_{p95}^{P_{w8}}$	$q_{med}^{P_{w8}}$	$q_{mean}^{P_{w8}}$	$q_{p95}^{P_{w8}}$
Ours	1.42	2.25	3.57	1.37	1.59	2.82
GNN.UP	1.47	2.00	3.85	<u>1.35</u>	<u>1.55</u>	<u>2.61</u>
SB.OP	<u>1.34</u>	<u>1.77</u>	<u>2.92</u>	1.38	1.58	2.66

Table 10: New engine: prediction accuracy of the new predictor.

6.2.1 Results on LCM’s accuracy. In the zero-shot setting (see Table 8), the effect of plan optimization is similar to that observed for other datasets. The GNN using optimized plans achieves 4.6% lower q_{med} for TPC-DS and 13.6% for Donor. Few-shot results (see Table 9) on TPC-DS and Donor also show patterns similar to those discussed in Sections 4.2 and 4.3. Specifically, both the LCMs’ accuracy and

the routings converge. For the zero-shot setup, q_{mean} is reduced by 8.1% for TPC-DS and by 26.3% for Donor. Finally, Table 10 reports the accuracy of the newly included predictor head. The observed metrics closely match those for the original predictor heads.

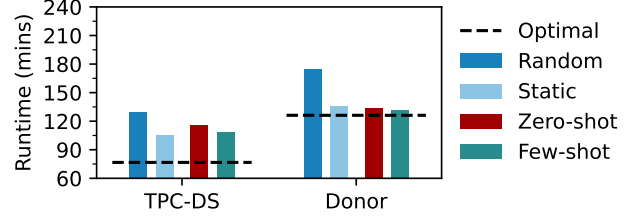


Figure 5: Query-level routing using our proposed LCM

6.2.2 Effect on Query Execution Times and Routing. Figure 5 shows the routing achieved with the proposed LCM. Using *zero-shot* predictors, the total runtime is reduced by 13.9 minutes (−10.8%) for TPC-DS and by 41.2 minutes (−23.6%) for Donor over random routing. In the *few-shot* setting, results show further improvements with 20.5 minutes (−15.9%) lower total runtime for TPC-DS and 42.6 minutes (−24.4%) for Donor. The fine-tuned predictors lead to a routing on-par with static routing.